

## Conventional and specially designed carotenoids: synthesis, optical properties and conductivity

S. Beutner, O. Gräf, K. Schaper, H.-D. Martin\*

Institute of Organic Chemistry, University of Düsseldorf, D-40225 Düsseldorf, Germany

**Abstract** - Conducting phenomena of carotenoids are explained by their lowest excited states. Little is known about the energies of these states, because the energies are hard to measure conventionally. In contrast, much information can be made available by dual fluorescence, energy transfer experiments, cyclovoltammetry and photoelectron spectroscopy. With this information available, new aspects are found that can contribute to explanations of conducting phenomena of carotenoids.

### DEEP COLOUR BY UTILIZING ACCEPTOR GROUPS

The phenomena of conductivity in carotenoids are often described using their lowest excited states. The knowledge of these states is equally important for the comprehension of numerous other properties, like the "antenna function" in the photosynthetic process, the quenching of excited chlorophylls in their triplet states, as well as the degradation of reactive or excited species of oxygen. There is a huge demand to determine and modify the location of these energy levels. Especially the lowering of these levels is important. That explains the demand for carotenoids with very bathochromic absorption bands. Besides creating these compounds by extending their chain length, one can also successfully introduce acceptor groups into the molecule.

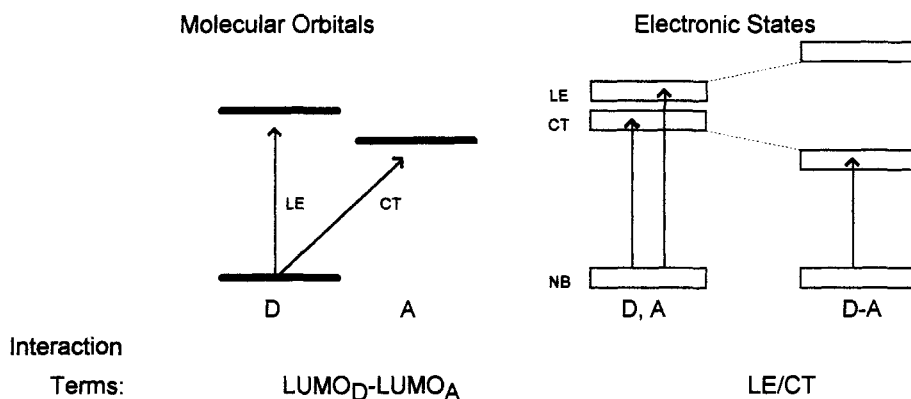


Fig. 1. Depression of excited states by acceptor-groups

These bathochromic shifts, achieved by introduction of fragments which act as acceptors, have been realized in dye chemistry for a long time. They are caused by the interaction of the  $LUMO_D-LUMO_A$  orbital fragments, leading to a depression of the excited states (Fig. 1.).

Figure 2 shows how the absorption band of longest wavelength of  $\beta$ -carotene 1b can significantly be shifted to longer wavelengths by introducing carbonyl acceptors (data for  $CHCl_3$ ).

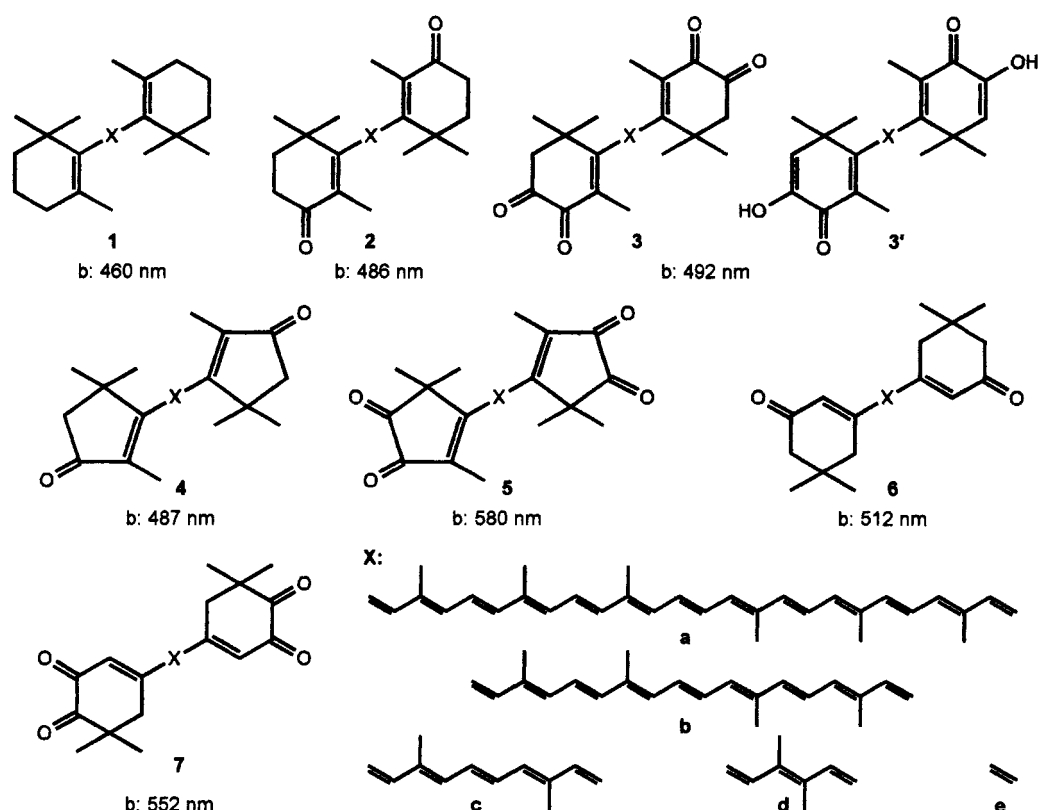


Fig. 2. The effect of carbonyl acceptor-groups

The bathochromic shift of 93 nm for the transition from 2,2'-dinorcanthaxanthin **4b** to violerythrin **5b** (ref. 1) indicates that implementation of 1,2-dicarbonyl fragments enables absorption bands of even longer wavelength. This is caused by the LUMO of the 1,2-dicarbonyl fragment, which is lower in energy. Therefore we used different oxidation methods to synthesize many carotenoids with 1,2-dicarbonyl fragments (e.g. **7b**, ref. 2). For compounds with absorption maxima at long wavelength other influences also have to be considered. For the series of conventional six-membered ring carotenoids for example, one does not observe a major bathochromic shift after insertion of dicarbonyl groups, due to the enolisation that leads to a diosphenol (e.g. **3'b**). This enolisation was prevented by shifting the dimethyl group from C-1 to C-2 (ref. 2). A further shift to longer wavelength is possible by reducing the steric interaction between ring and side-chain, which was accomplished after the 18-methyl-group was removed. In such compounds the less distorted *s-trans* conformation is favoured.

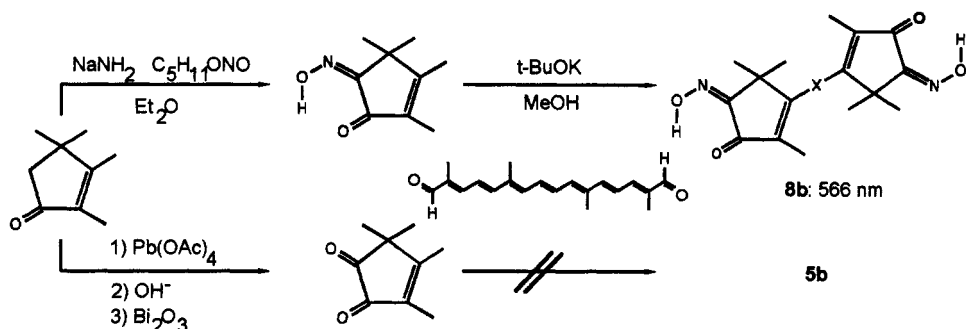


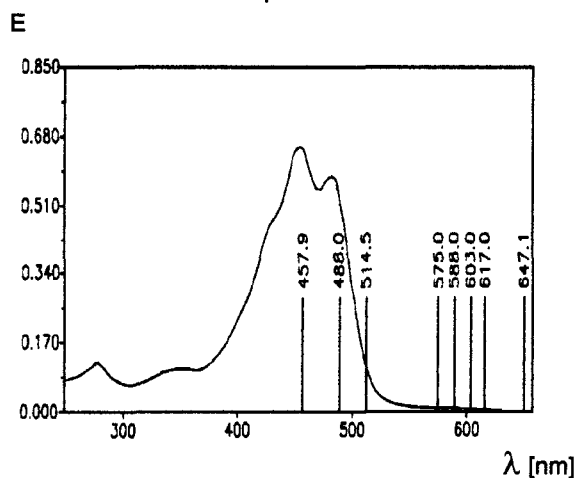
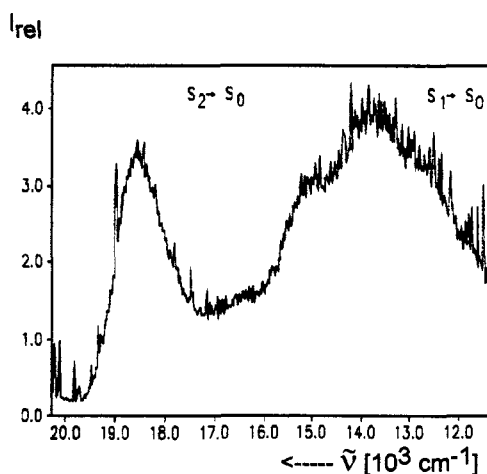
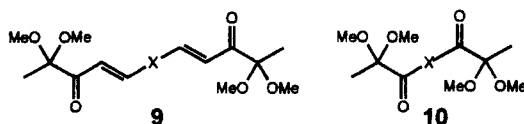
Fig. 3. The aldol condensation route to violerythrin dioxime **8b**

Another way to synthesize bathochromic-absorbing compounds leads to the introduction of oxime-groups. New synthetic ways are also possible for these groups, as shown by the aldol condensation route to violerythrin dioxime **8b** (Fig. 3, ref. 3).

## SINGLET STATES IN SOLUTION

The location of the  $S_1$  and  $T_1$  states of carotenoids with  $C_{2h}$ -symmetry cannot be determined by conventional absorption spectroscopy. The visible transition with the lowest energy refers to the  $S_0$ - $S_2$  excitation ( ${}^1A_g \rightarrow {}^1B_u$ ). The  $S_1$  state has the same  $A_g$  symmetry as the ground state so that the  $S_0$ - $S_1$  excitation is prohibited by symmetry. Even fluorescence spectroscopy of carotenoids with long chains like  $\beta$ -carotene **1b** does not provide more information about the  $S_1$  state (ref. 4). As shown experimentally, only short carotenoids with less than nine double bonds fluoresce from the  $S_1$  state. Compounds with longer chains on the other hand exhibit anti-Kasha emission from the  $S_2$  state (ref. 5). In some special cases dual fluorescence, i.e. simultaneous emission from  $S_1$  and  $S_2$  states, was observed (refs. 5,6). In the fluorescence spectrum of compound **9c** two fluorescence maxima at  $18492\text{ cm}^{-1}$  (540 nm) and  $13600\text{ cm}^{-1}$  (735 nm) were found (Fig. 5, ref. 7).

The explanation of this result as being caused by dual fluorescence is confirmed by other findings. The low energy fluorescence for instance is also observed after irradiation with light of longer wavelength than needed for  $S_0$ - $S_2$ -excitation. Also the emission band of longer wavelength disappears at low concentrations ( $10^{-7}$  to  $10^{-8}$  M). Thus the observed fluorescence does not emanate from one single excited state. A simultaneous existence of excimer and monomer fluorescence is furthermore unlikely due to the non-linear dependence on the concentration.

Fig. 4. Absorption spectra of **9c** ( $\text{CHCl}_3$ )Fig. 5. Fluorescence spectra of **9c** ( $\text{CHCl}_3$ )

The fact that the  $S_2$ - $S_0$ -fluorescence band is not a mirror image of the  $S_0$ - $S_2$ -absorption band indicates that there are different geometries present in  $S_0$  and  $S_2$ . The 0-0 transition of the  $S_2$ - $S_0$ -fluorescence is in the range of  $19200$ - $19500\text{ cm}^{-1}$  (520-512 nm). Based on fluorescence excitation spectra the band at  $16200\text{ cm}^{-1}$  is attributed to the origin of the  $S_1$ - $S_0$  band. The  $S_2$ - $S_1$  energy gap thus amounts to merely  $3000$ - $3300\text{ cm}^{-1}$ . This is a remarkably small value because dual fluorescence is usually associated with a larger energy difference. For compound **10b**, which contains eleven  $\pi$ -bonds like  $\beta$ -carotene **1b** and also shows dual fluorescence, an  $S_2$ - $S_1$  energy gap of  $3400$ - $4000\text{ cm}^{-1}$  is measured. This confirms that the  $S_2$ - $S_1$  energy gap in these two cases grows bigger with increasing chain length. While the  $S_0$ - $S_2$  energy gap decreases at the same time, the  $S_0$ - $S_1$  energy gap diminishes even more. For  $\beta$ -carotene **1b** several  $S_2$ - $S_1$  gap values have been proposed (ref. 5).

## TRIPLET STATES IN SOLUTION

The location of the  $T_1$  state cannot be determined by emission spectroscopy because phosphorescence has not yet been observed. An estimate of the location of triplet states is possible by using energy transfer experiments. It is known that carotenoids physically deactivate  ${}^1\text{O}_2$  extremely efficiently (ref. 8). For this quenching the following mechanism is assumed:



The excitation energy of  ${}^1\text{O}_2$  is transferred to the carotenoid in a bimolecular energy-transfer reaction. This energy is given off by the carotenoid as thermal energy. This energy transfer occurs especially efficiently if the triplet level of the carotenoid lies below the excitation energy of  ${}^1\text{O}_2$  ( $1270 \text{ nm} \cong 7.9 \cdot 10^3 \text{ cm}^{-1} \cong 94 \text{ KJ mol}^{-1}$ ).

The rate of  ${}^1\text{O}_2$  depletion is, for example, monitored by the decreasing emission of  ${}^1\text{O}_2$  at  $1270 \text{ nm}$ . The rate increases with addition of carotenoids. Rate constants for the quenching reaction can be determined for different carotenoids by employing a Stern-Volmer relation (ref. 9).

Figure 6 contains a plot of rate constants for the quenching, determined as described above, versus the singlet excitation energies  $S_0$ - $S_2$  of the carotenoids. It shows the usual image for a bimolecular energy-transfer process. For carotenoids with singlet excitation energies of ca.  $22.2 \cdot 10^3 \text{ cm}^{-1}$  or more an additional thermal energy is needed. There the rate constants for the quenching increase with the thermal energy  $kT$ . In these cases the triplet levels of the carotenoids are above  $94 \text{ KJ mol}^{-1}$ . For carotenoids with smaller excitation energies the triplet levels are below this value, so that the energy transfer does not require additional thermal energy and tends to be limited by diffusion. This idea is supported by the fact that for  $\beta$ -carotene **1b**, which can be found at the bend of the graph, a triplet energy comparable to that of  ${}^1\text{O}_2$  is discussed (ref. 8).

Because the triplet levels of the carotenoids participate in the process of energy transfer, and since the measured excitation energies are determined by  $S_2$ , Fig. 6 can be evaluated as an argument for a linear connection of  $S_2$  and  $T_1$  states. Such a connection is also reached by theoretical considerations. It is known that the absorption band of longest wavelength of carotenoids is a function of their effective chain length  $N$  (ref. 10).

$$\lambda^2 = 38.60 - 40.72 \cdot 0.920^N [10^4 \text{ nm}^2] \Rightarrow \tilde{\nu} = 77.75 \cdot 1/N + 14.09 [10^3 \text{ cm}^{-1}]$$

for  $N = 9$  to  $20$ ,  $r = 0.99999$

The carotenoids shown in Fig. 6 possess effective chain lengths  $N$  between 9 and 20. In this area the singlet excitation energies are proportional to the reciprocal chain lengths. Such a connection is also assumed for the triplet levels (refs. 11,12).

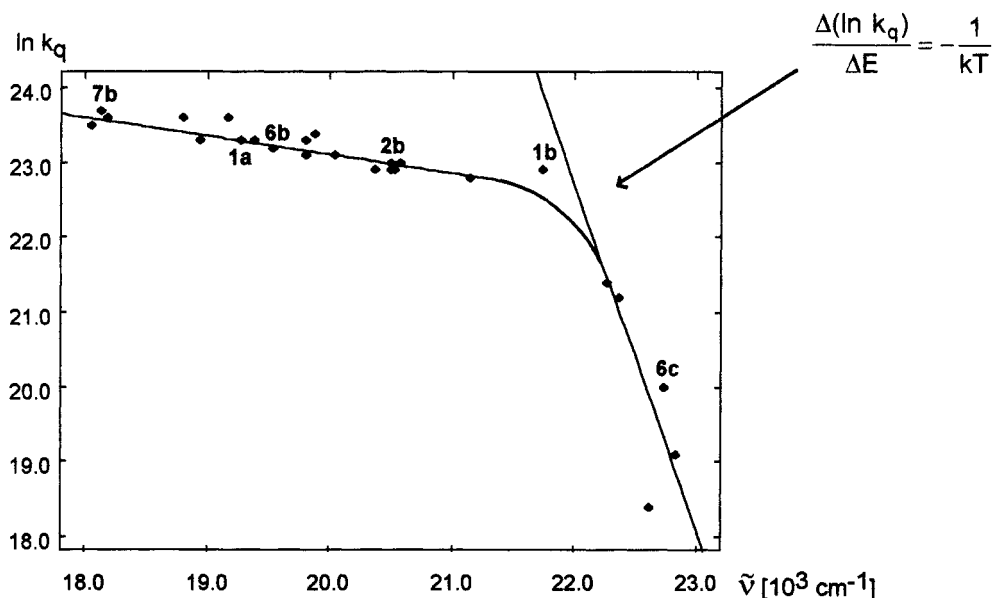


Fig. 6.  $\ln k_q$  versus  $S_0$ - $S_2$  excitation energy for different carotenoids

Since there exists only contradictory and speculative data for triplet energies of some carotenoids, a quantitative transfer of the measured singlet energies to triplet energies does not seem justified yet.

## HOMO ENERGIES IN SOLUTION

Information about the energetic position of higher states is not only obtainable from absorption and emission spectra. Electrochemical investigations also deliver information about redox potentials and the relative location of states in energy. Cyclovoltammograms of  $\beta$ -carotene **1b** and its homologues (**1a**, **1c**, **1d**) show that the number of possible redox steps increases with longer chain lengths while the redox potentials are shifted to lower energies (ref. 13). The electron transfer steps for charging or discharging of the carotenoids are two very close one-electron transfer steps. This can also be thought of as filling and emptying of molecular orbitals. The first oxidation potentials should therefore be proportional to the HOMO-energies. In the series of  $\beta$ -carotenoids **1a-d** one would assume from theoretical considerations that with increasing chain length  $n$  an increase of the HOMO by  $1/n$  is expected. The first oxidation potentials correlate with  $1/n$  (ref. 13).

Furthermore, the potential difference between the first oxidation step and the first reduction step is explained as the electrochemical HOMO-LUMO energy gap. These energy gaps also correlate with  $1/n$  (Fig. 7,  $E(\text{gap})=9.7/n+1.25$  [eV]).

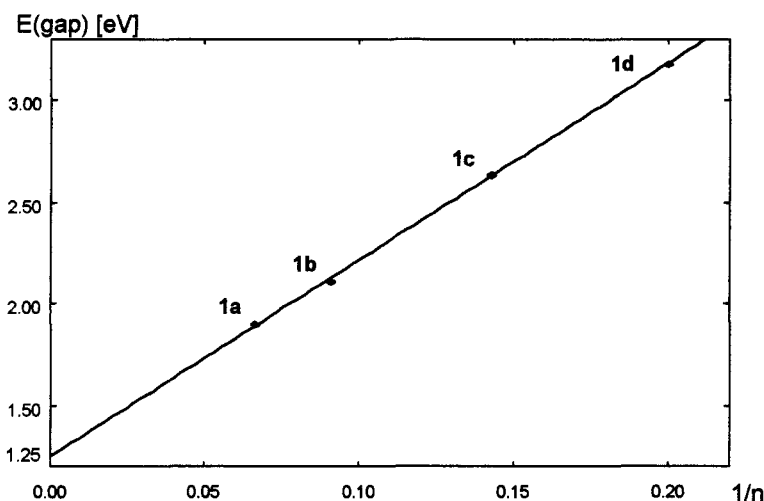


Fig. 7. Electrochemical HOMO-LUMO energy gap of carotenoids versus the reciprocal chain length

It is remarkable that with extrapolation to infinite chain length a gap of 1.25 eV is expected. This value fits into the area of energy gaps proposed for polyacetylene (1.24-1.28 eV, ref. 14). The steady change in HOMO and LUMO energies shows that these energies are subject to continual changes with the chain length.

## HOMO ENERGIES IN THE SOLID STATE

For the interpretation of conducting phenomena of carotenoids, their solid-state properties have to be considered. Following Koopmans' theorem, the solid-state HOMO energies can be calculated from threshold energies  $I^{\text{th}}$  (ref. 15). The threshold energies of solid materials can be measured by solid state photoelectron spectroscopy (ref. 16). Compared to the gas phase, the ionization in the solid state needs less energy because of the polarization of the surrounding matter (Fig. 8).

The carotenes **1a-d** show, just as in solution (*vide supra*), a rise in HOMO energy when the chain length is increased. There is a good correlation between the threshold energies in the solid state and the oxidation half-wave potentials in solution (Table 1, Fig. 9, ref. 17). Considering these results, a transfer of solution and gas-phase findings to the solid state seems justified.

Another justification can be found by considering carotenoids with the same chain length, but different end-groups. It is found that the introduction of carbonyl and 1,2-dicarbonyl acceptor fragments into the end-group leads to a lowering of the HOMO energy (**4b/5b**).

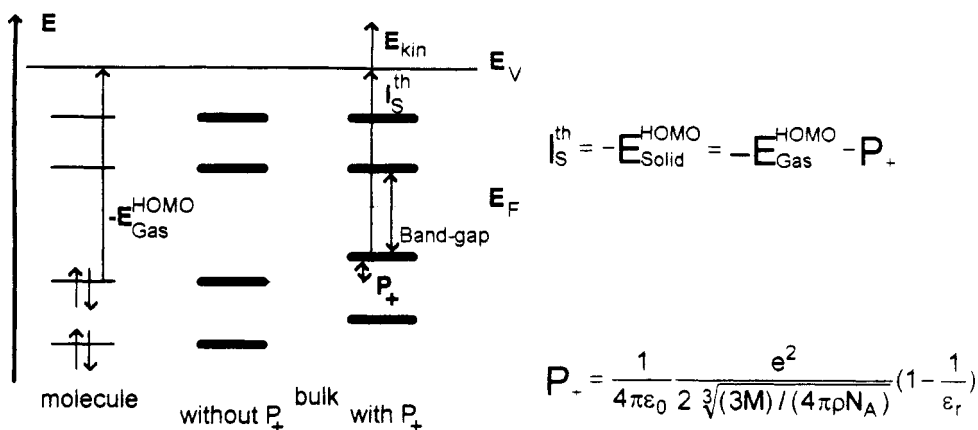


Fig. 8. Illustration of the energy levels

TABLE 1. HOMO-Energies

| Carotenoid | $E_{1/2}^{Ox}$ [mV] | $I_S^{th}$ [eV] |
|------------|---------------------|-----------------|
| 1d         | 820                 | 4.42            |
| 1c         | 670                 | 4.02            |
| 1b         | 510                 | 3.88            |
| 1a         | 430                 | 3.84            |
| 4b         | %                   | 5.89            |
| 5b         | %                   | 7.06            |

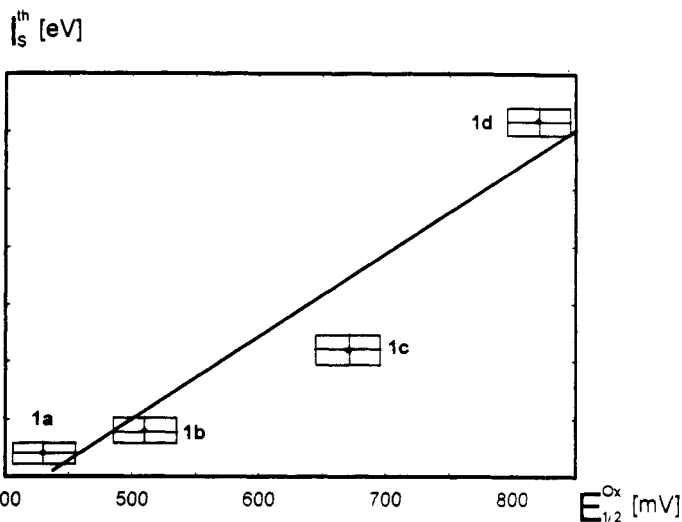


Fig. 9. Threshold energies versus oxidation potentials

This is in accord with quantum mechanical calculations for the gas-phase ionization potential of systems with shorter wavelengths. The "mini-violerythrin" **5e** has a 0.42 eV higher ionization energy than the diketone **4e**. This effect, provoked by the introduction of acceptor fragments, is also observed in the solid state, therefore showing that these fragments are responsible for an even greater lowering of the LUMO energy and therefore for a bathochromic shift.

## CONDUCTIVITY

The fact that carotenoids on the one hand have remarkably low threshold energies for ionization ( $\beta$ -carotene **1b**: 3.9 eV or 310 nm), and, on the other hand, show at least one forbidden singlet-singlet transition ( $S_0$ - $S_1$ ,  $1^1A_g$ - $2^1A_g$ ) in the range of about 600-800 nm, may be closely related to the photoconductivity of these compounds (ref. 18). The generation of charge-carriers is a consequence of excitation into low-lying, nonconducting excitation states. These states need not necessarily be the same as those in the absorption spectra. A close resemblance of absorption spectra to photoconductivity excitation spectra is a strong indication of surface charge-carrier generation, otherwise bulk photoconductivity has to be assumed.

The photoconductivity excitation spectra of  $\beta$ -carotene (Fig. 10) display obviously bulk photoresponse under conventional irradiation with wavelengths around 300-400 nm and 600-900 nm (refs. 18,19). Surprisingly, in laser-induced conductivity experiments, no effect has been recorded at 640 nm (ref. 20).

The polarity of the illuminated electrodes (in sandwich-type cells) is of importance: photocurrents are higher if the irradiated electrode is positive. An interpretation within the band model has been given using a suitable band deformation (ref. 19). The involvement of a low-lying triplet state in the photoconductivity in the region 600-800 nm was proposed (ref. 18). This assumption however is questionable since the  $S_0-T_1$  transition probably occurs at longer wavelengths. As mentioned above the  $S_1(2^1A_g)$  state has to be assigned to the range 600-800 nm. Thus, the role of this singlet state in photoconductivity is still unknown and must be elucidated.

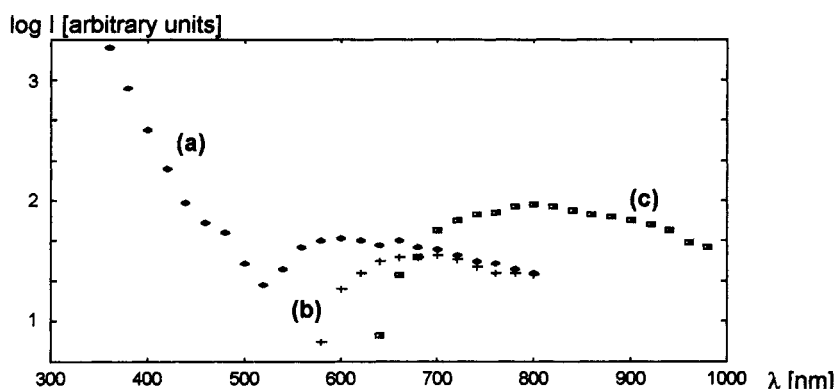


Fig. 10. Photoconductivity spectra of  $\beta$ -carotene sandwich-type cell (Cr/Car/Cr) and surface type sample. (a) Spectra when positive electrode is illuminated, (b) spectra when negative electrode is illuminated, (c) surface-type sample spectra (ref. 19).

Both photoconductivity and dark DC conductivity are thermally activated,  $E_a=0.2-0.4$  eV (photo) and  $E_a=1.4-1.6$  eV (dark) (refs. 21,22). The dark DC conductivity is strongly increased by adsorbed gases (alcohols, amines, oxygen) (refs. 21,23). Increases in current by factors of  $10^6$  are observed. This has been interpreted in terms of reduced activation energies.

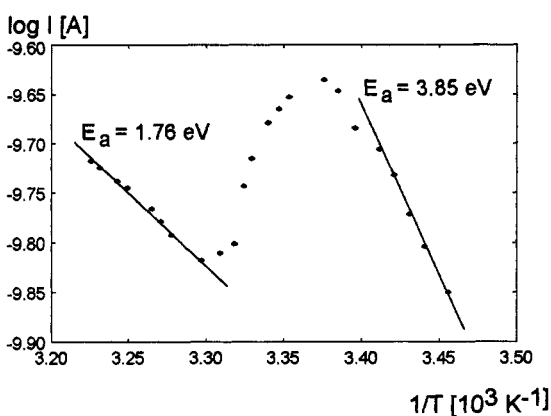


Fig. 11 Semiconductivity in an ethyl acetate powder cell of 15,15'-*cis*- $\beta$ -carotene as a function of temperature (ref. 25).

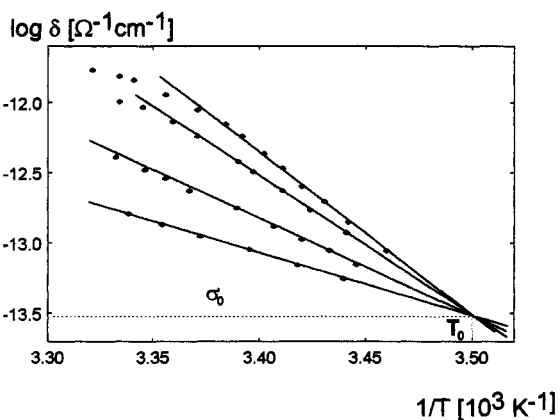


Fig. 12. Semiconductivity data for 15,15'-*cis*- $\beta$ -carotene powder cell with the absorption of different amounts of ethyl acetate vapour (ref.25).

Several carotenoids show the compensation effect (refs. 24,25): in the conductivity equation  $\sigma(T)=\sigma_0 \exp(-E_a/2kT)$ , the pre-exponential factor  $\sigma_0$  is also dependent on the activation energy,  $\sigma_0=\sigma_0' \exp(+E_a/2kT_0)$ . It is remarkable that the compensation rule is valid for 15,15'-*cis*- $\beta$ -carotene (Figs. 11,12) but not in all-*trans*- $\beta$ -carotene! The latter responds to adsorbed gases, but this is an effect on  $E_a$ , not on  $\sigma_0$ .

The energy state diagram of  $\beta$ -carotene is still a matter of debate. The proposal given in the context of photoconductivity (ref. 18) obviously needs revision. Useful information is obtained from quenching studies (ref. 8 and Fig. 6). In addition, the ionization threshold of solid  $\beta$ -carotene at 3.9 eV (ca. 310 nm) should be taken into account (Table 1). In Fig. 13 a revised but still approximate energy level diagram is depicted.

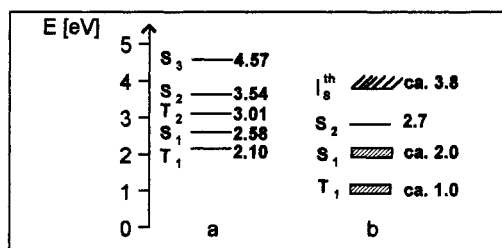


Fig. 13. Previous (a) and revised (b) approximate energy diagram of  $\beta$ -carotene

The most promising devices in future developments with carotenoids will probably comprise gas sensors, optical switching devices and solid state batteries (ref. 26). Deeply coloured and bathochromic absorbing carotenoids (e.g. **5b**, **7b**, **8b**) may change the usual photoconductivity excitation spectra considerably and we are therefore currently investigating these phenomena.

Another area of useful application can be the incorporation of electroactive carotenoids (caroviologens) into vesicle membranes (ref. 27) and the preparation of Langmuir-Blodgett films containing amphiphilic carotenoids (ref. 28).

#### ACKNOWLEDGEMENT

We gratefully appreciate financial support by the Deutsche Forschungsgemeinschaft, the Fonds der Chemischen Industrie and BASF AG as well as the efficient collaboration with Prof. Heinze, Freiburg, Dr. Paust, BASF AG, Dr. Bettermann, Prof. Mootz, Prof. Sies and Prof. Strehblow, Düsseldorf.

#### REFERENCES

1. F. Kienzle and R.E. Minder, *Helv. Chim. Acta* **59**, 439-453 (1976)
2. S. Röver, Dissertation, Universität Düsseldorf (1988), D. Baltschun, Dissertation, Universität Düsseldorf (1992)
3. D. Elsässer, W. Langensiepen, H.-D. Martin, to be published
4. T. Gillbro and R.J. Cogdell, *Chem. Phys. Lett.* **158**, 312-316 (1989)
5. R. Snyder, E. Arvidson, C. Foote, L. Harrigan and R.L. Christensen, *J. Am. Chem. Soc.* **107**, 4117-4122 (1985); P.O. Andersson, T. Gilbro, A.E. Asato and R.S.H. Liu, *J. Lumin.* **51**, 11-20 (1992); R.J. Thrash, H.L.B. Fang and G.E. Leroi, *J. Chem. Phys.* **67**, 5930-5933 (1977)
6. M. Mimuro, Y. Nishimura, I. Yamazaki, T. Katoh and U. Nagashima, *J. Lumin.* **51**, 1 (1992)
7. H. Bettermann, M. Bienioschek, H. Ippendorf and H.-D. Martin, *Angew. Chem. Int. Ed. Engl.* **31**, 1042-1044 (1992), *J. Lumin.* in press
8. P.F. Conn, W. Schalch and T.G. Truscott, *J. Photochem. Photobiol. B: Biol.* **11**, 41-47 (1991); T.G. Truscott, *ibid.* **6**, 359-371 (1990)
9. T.P.A. Devasagayam, T. Werner, H. Ippendorf, H.-D. Martin and H. Sies, *Photochem. Photobiol.* **55**, 511-514 (1992)
10. K. Hirayama, *J. Am. Chem. Soc.* **77**, 373-379, 379-381, 382-383, 383-384 (1955)
11. R. Bensasson, E. J. Land and B. Maudinas, *Photochem. Photobiol.* **23**, 189 (1976)
12. P. Mathis, Thesis, Orsay (1970)
13. O. Gräf, J. Heinze, H.-D. Martin and A. Smie, to be published
14. J.L. Bredas, R. Silbey, D.S. Boudreaux and R.R. Chance, *J. Am. Chem. Soc.* **105**, 6555-6559 (1983)
15. G. Ertl and J. Küppers, *Low Energy Electrons and Surface Chemistry*, p. 87, VCH Verlagsgesellschaft, Weinheim (1985)
16. T.B. Tang, K. Seki, H. Inokuchi and T. Tani, *J. Appl. Phys.* **59**, 5-10 (1986)
17. K. Schaper, Dissertation, Universität Düsseldorf (1993)
18. J.O. Williams, in *Carotenoids as Colorants and Vitamin A Precursors* (J.C. Bauernfeind, ed.), pp. 787-813, Academic Press, New York (1981)
19. Y. Hoshino and K. Tateishi, *J. Phys. Soc. Jpn.* **46**, 72-76 (1979)
20. M. Tierney and D.M. Lubman, *Appl. Spectrosc.* **42**, 1073-1078 (1988)
21. T.N. Misra, B. Rosenberg and R. Switzer, *J. Chem. Phys.* **48**, 2096-2102 (1968)
22. L. Brehmer and H. Hänsel, *Z. Phys. Chem.* **258**, 925-936 (1977)
23. T.G.J. van Oirschoot, D. van Leeuwen and J. Medema, *J. Electroanal. Chem.* **37**, 373-385 (1972)
24. B. Mallik, A. Ghosh and T.N. Misra, *Jpn. J. Appl. Phys.* **19**, 207-208 (1980)
25. B. Mitra and T.N. Misra, *Jpn. J. Appl. Phys.* **26**, 66-69 (1987)
26. P. Pal and T.N. Misra, *Indian J. Phys.* **65B**, 459-465 (1991)
27. T.S. Arrhenius, M.B. Desce, M. Dvořaitzky, J.M. Lehn and J. Malthete, *Proc. Natl. Acad. Sci. USA* **83**, 5355-5359 (1986)
28. A. Wegmann, B. Tieke, J. Pfeiffer, and B. Hilti, *J. Chem. Soc. Chem. Commun.*, 586-588 (1989)